A Concave Fluorescent Sensor for Anions Based on 6-Methoxy-1-methylquinolinium

Valeria Amendola, Luigi Fabbrizzi,* and Enrico Monzani[a]

Abstract: The ligand **2**, in which three fluorogenic 6-methoxy-1-methylquinolinium fragments are appended to a mesityl platform, in MeCN forms 1:1 adducts with halides and other inorganic anions. ^{1}H NMR studies and molecular modelling indicate that **2** provides a cavity for anion inclusion and establishes electrostatic interactions with the guest. Anion inclusion induces quenching of the fluorogenic fragments with an efficiency decreasing along the series $Br^- \gg I^- > NCS^- \gg Cl^- > NO_3^- > HSO_4^-$. The fluorimetric response of **2** to anions is orders of magnitude more sensitive than that of just 6-methoxy-1-methylquinolinium, ligand **1**.

Keywords: anions · fluorescence spectroscopy · molecular recognition · receptors · sensors

Introduction

A variety of fluorophores exist that do not interact firmly with the desired substrate, but give rise to occasional collisions, which may lead to the quenching of the fluorophore emission. This behaviour is typically regulated by the Stern–Volmer equation: $I_o/I = 1 + k_q\tau_o[A] = 1 + K_{SV}[A]$, whose plot makes it possible to determine quantitatively, over a wide range, the concentration of analyte A from the measured fluorescence intensity I.[1]

A classical fluorophore typically used in Stern–Volmer titrations is 6-methoxy-1-methylquinolinium (**1**), which, being positively charged, is suitable for interaction with anions, and is currently employed for the detection of halides (in particular chloride) in various media.[2,3] On excitation of a solution of **1** at $\lambda = 330$ nm, a rather intense emission band develops at 440 nm. This band is quenched more or less completely on addition of anions, depending upon the pertinent K_{SV} value.

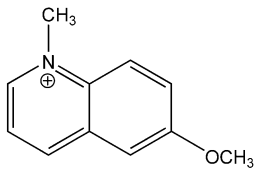

1

Systems operating with a Stern–Volmer behaviour, even if useful in particular circumstances, have to be considered rather primitive sensing devices for analytes, whether charged or not. For several years, interest has developed for the design of more sophisticated molecular systems (receptors, R) capable of strongly interacting with the envisaged analyte (A), giving rise to an adduct with 1:1 stoichiometry, characterised by a definite association constant K_{ass} (related to the equilibrium: $R + A \rightleftharpoons [R{\cdot}A]$). Such receptors must contain multiple interaction sites for the analyte, symmetrically positioned within their framework.[4,5] If the analyte is an anion, these sites could be positively charged groups. Following this, we synthesised system **2**, in which three 6-methoxy-1-methylquinolinium fragments have been implanted on a mesityl platform. The 1,3,5-functionalised benzene scaffold has been frequently used in order to build up a variety of receptors.[6,7] In particular, system **2** possesses three symmetrically placed positive charges and, as suggested by molecular modelling, may generate a cavity suitable for anion inclusion.

It will be shown that **2** behaves as an efficient receptor for anions, giving rise to 1:1 adducts, whose $\log K_{ass}$ values, determined through spectrophotometric and ^{1}H NMR titrations in MeCN, vary from 4.55 (for Cl^-) to 3.40 (for NCS^-). Most interestingly, the spectrofluorimetric response of **2** is remarkably enhanced relative to that of 6-methoxy-1-methylquinolinium alone. In particular, I_0/I versus [anion] plots of a much higher slope (and sensitivity) are produced, which fit Stern–Volmer type equations containing both K_{SV} and K_{ass} parameters.

[a] Dr. V. Amendola, Prof. L. Fabbrizzi, Dr. E. Monzani
Dipartimento di Chimica Generale
Università di Pavia
via Taramelli 12, 27100 Pavia (Italy)
Fax: (+39) 0382-528544
E-mail: luigi.fabbrizzi@unipv.it

DOI: 10.1002/chem.200305338

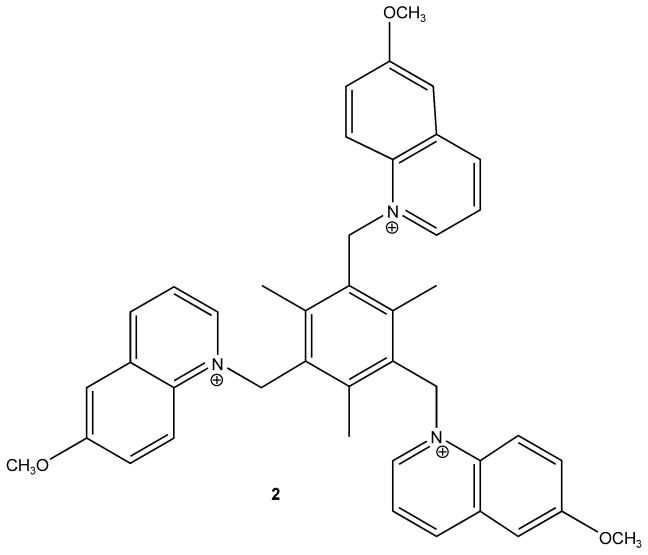

2

Results and Discussion

Spectrophotometric determination of the association constants with anions: Reversible binding of a given anion X^- with the receptor **2** was investigated in MeCN , at 25 °C, by means of spectrophotometric titration experiments. The 6-methoxy-1-methylquinolinium fragment possesses push-pull features that give rise to a charge-transfer transition in the UV region. It is expected that the electrostatic interaction of an anion with the positively charged nitrogen atoms alters the dipole, thus modifying the absorption spectrum.

Indeed, this is observed with most of the investigated anions. As an example, Figure 1 illustrates the family of spectra obtained when a solution of **2** in MeCN (4×10^{-4} M) is titrated with a standard solution of benzyltributylammonium bromide. The presence of two distinct isosbestic points indicates that only two species are present at equilibrium. The inset in Figure 1 shows the increase of the absorbance at 344 nm on progressive addition of Br^- (as equivalents). This titration profile clearly indicates the formation of an adduct of 1:1 stoichiometry. Nonlinear least-squares treatment of spectral data (using the HYPERQUAD program)[8] gave an association constant K_{ass} of 4.42 ± 0.04 log units for the equilibrium given in Equation (1):

$$\mathbf{2}^{3+} + Br^- \rightleftharpoons [\mathbf{2}\cdot Br]^{2+} \quad (1)$$

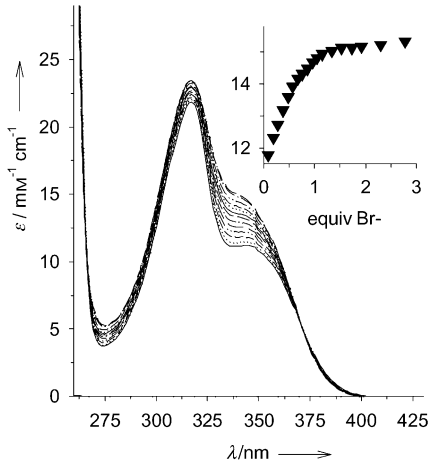

Figure 1. UV/Vis titration of **2** (4×10^{-4} M) with a standard solution of Br^-, in MeCN; the addition of the anion makes the absorption of the bands of the receptor increase (in particular at 340 nm). Inset: titration profile (molar absorbance of **2** at 340 nm vs equivalents of bromide).

Spectral changes and titration profiles indicating the formation of 1:1 adducts were obtained for a variety of anions: corresponding values of $\log K_{ass}$ are reported in Table 1. Titration with perchlorate and triflate anions did not induce any spectral changes indicating no or extremely weak interaction with $\mathbf{2}^{3+}$.

Table 1 indicates that the investigated receptor displays the highest affinity towards chloride. Looking at the three studied spherical anions (halides), the affinity decreases along the series $Cl^- > Br^- > I^-$, that is, with the charge density on the substrate, a trend that demonstrates the dominating role of the electrostatic interaction. Among polyatomic anions, NO_3^- and HSO_4^-, which display similar K_{ass} values, offer three oxygen atoms with partially negative charges that may fit with the array of the three positive charges of the quinolinium groups of the receptor. The lowest affinity is observed with the rodlike triatomic anion NCS^-.

Table 1. Association constants K_{ass} between **2** and anions in MeCN.

Anion	**2**/logK_{ass}[a]	**2**/logK_{ass}[b]
Cl^-	4.55 ± 0.03	4.64 ± 0.06
Br^-	4.42 ± 0.04	4.28 ± 0.05
I^-	3.48 ± 0.01	
NO_3^-	3.91 ± 0.03	
HSO_4^-	3.79 ± 0.02	
NCS^-	3.40 ± 0.02	
ClO_4^-	<2	
$CF_3SO_3^-$	<2	

[a] Constants were calculated by nonlinear least-squares treatment of spectrophotometric data at 25 °C in MeCN. [b] Constants were calculated by nonlinear least-squares treatment of ^{1}H NMR titration data at 25 °C in CD_3CN.

It has to be noted that titration of 6-methoxy-1-methylquinolinium (**1**) with the same family of anions did not induce any spectral modification, even after the addition of a large excess of anion, indicating no formation of an adduct or ion-pair. Thus, it appears that the presence of three pre-positioned quinolinium groups is essential for the formation of a solution stable complex.

^{1}H NMR titration experiments: For chloride and bromide anions, titration experiments were carried out in CD_3CN at 25 °C and followed by ^{1}H NMR analysis. A standard solution of the benzyltributylammonium salt (chloride or bromide) in CD_3CN was progressively added to a solution of **2** in CD_3CN.

Some representative spectra collected during the titration with chloride are reported in Figure 2. The most remarkable shifts are assigned to the H3 and H4 atoms. In particular, on

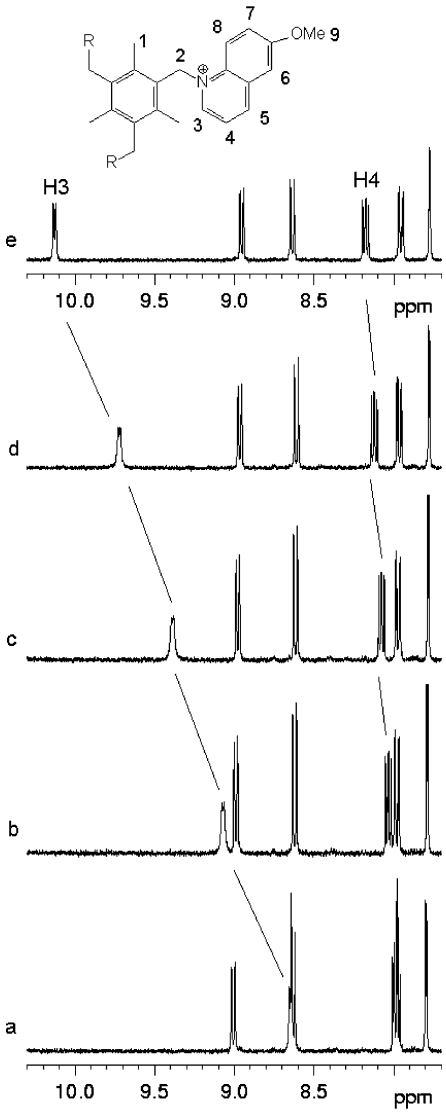

Figure 2. ^{1}H NMR spectra of the solution containing **2** and a) 0, b) 0.3, c) 0.6, d) 0.9 and e) 2.5 equivalents of chloride (25 °C, CD_3CN).

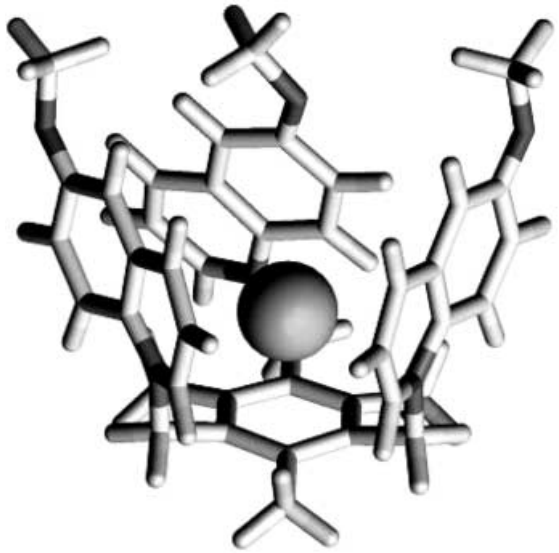

Figure 3. Molecular model of the $[\mathbf{2}\cdot Cl]^{2+}$ adduct obtained by the AMBER program.

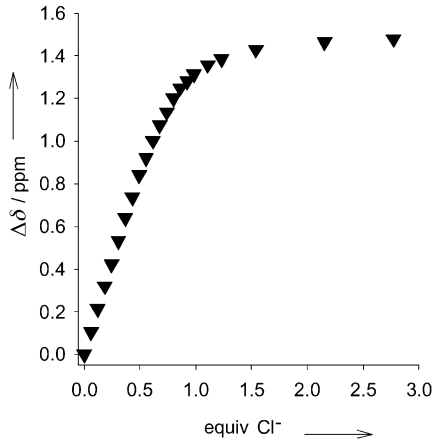

Figure 4. Titration profile of **2** with a standard solution of chloride (variation of the chemical shift of H3 vs equivalents of Cl^-).

addition of Cl^-, the H3 signal undergoes a downfield shift of about 1.5 ppm ($\Delta\delta$), reaching a limiting value of $\delta =$ 10.15 ppm. The downfield shift of H4 is a more moderate value of 0.2 ppm. These features can be accounted for by considering that, on titration, **2** folds its 6-methoxy-1-methylquinolinium arms to give a cavity for anion inclusion. In these circumstances, each H3 atom feels an electrostatic field of increased positive charge, which induces the downfield shift. Such an effect is lower for H4 atoms, which are farther from the positive electrical charges. These results point towards a stereochemical arrangement in which **2** has adopted the shape of a bowl, containing the chloride ion.

Such a hypothesis is supported by molecular modelling. In particular, molecular mechanics calculations, using the AMBER package,[9] produced the model structure shown in Figure 3: in the model, the receptor is arranged in such a way to generate a well-defined cavity and the chloride ion stays inside the bowl, close to the positively charged nitrogen atoms.

Figure 4 reports the variation of the chemical shift of H3 versus the equivalents of Cl^-. The titration profile confirms the formation of a 1:1 adduct, whose K_{ass}, calculated through least-squares nonlinear fitting, is 4.64 ± 0.06 log units. This is in excellent agreement with the value calculated from the spectrophotometric titration.

Similar behaviour was observed on titration of **2** with a benzyltributylammonium bromide standard solution. The distinct downfield shift of the H3 signal was also observed, but its limiting value was lower than that found for chloride: $\delta = 9.91$ ppm. This may be due to the fact that the larger bromide ion induces the formation of a more open cavity, in which the quinolinium centres are farther from each other. Again, the H3 chemical shift versus equivalents of bromide profile indicates the formation of a complex of 1:1 stoichiometry, with $\log K_{ass} = 4.28 \pm 0.05$, in good agreement with the value obtained from spectrophotometric titrations. It has to be noted that trifurcated receptors based on the mesityl

core, whose side-chains contain the pyridinium fragment and a variety of appendages, have been investigated by ^{1}H NMR titrations and a similar sequence of association constants was found with halide ions.[11]

Spectrofluorimetric studies: As far as the fluorimetric response is concerned, it seemed initially convenient to investigate the quenching of **1** when titrated by inorganic anions in MeCN.

Figure 5 reports the I_0/I values versus the concentration of the added anion (I_0: fluorescence intensity before anion addition; I: fluorescence intensity during the addition). The Stern–Volmer [Eq. (2)] equation fits the data well:

$$I_0/I = 1 + k_q\tau_0[Q] = 1 + K_{SV}[Q] \quad (2)$$

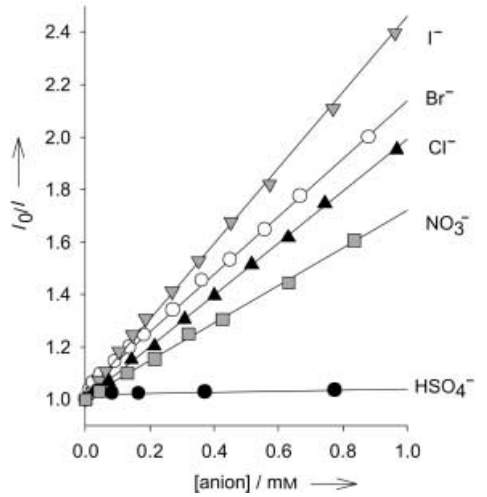

Figure 5. Stern–Volmer profiles obtained from the spectrofluorimetric titrations of **1** with different anions.

as indicated by the least-squares straight lines in the figure. Values of the Stern–Volmer constants K_{SV} obtained from the fitting are reported in Table 2.

It is observed that among halides K_{SV} decreases along the series $I^- > Br^- > Cl^-$. This behaviour may be generically ascribed to the "heavy atom effect".[10] However, if the fluorescence-quenching is associated with the occurrence of an electron-transfer process from the anion to the excited fluorophore, the sequence parallels the reducing tendencies of the halide ion. In this context, it has to be noted that a relatively high value of K_{SV} is observed also for the NCS^- ion, which displays distinct reducing tendencies ((NCS/NCS^-) potential: −1.50 V vs NHE).[12]

In the case of **2**, I_0/I versus [anion] plots do not fit the simple Stern–Volmer equation [Eq. (2)]. Because the fluorophore (receptor) and quencher (anion) form stable 1:1 adducts, more than just occasional collisions must be occurring. Under these circumstances, we can consider two different cases.

First we will consider the case in which the the 1:1 adduct is not fluorescent at all (i.e., the emission of the receptor–fluorophore has been completely quenched by the included anion). In this case, we can make use of Equation (3):[13]

$$I_0/I = (1 + K_{SV}[Q])(1 + K_{ass}[Q]) \quad (3)$$

This parabolic behaviour is shown by the anions I^-, NCS^- and Br^- (see Figure 6).

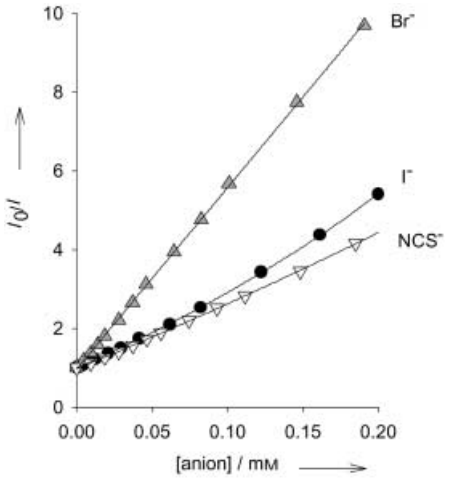

Figure 6. I_0/I profiles for the titrations of **2** with Br^-, I^- and NCS^-.

Pertinent K_{SV} and K_{ass} values, obtained through nonlinear fitting on Equation (3), are reported in Table 2. K_{ass} values obtained from spectrofluorimetric data are in good agreement with those obtained through spectrophotometric titration experiments and reported in Table 1. Quite surprisingly, the Br^- ion shows a linear, rather than a parabolic curve: this is due to the fact that, at the investigated concentration of quencher, $1 + K_{SV}[Q] \approx 1$. As a consequence, the slope of the linear plot should correspond to the association constant K_{ass}. The agreement is not perfect, but satisfactory: $\log K_{ass}$ fluorimetric: 4.55 ± 0.05, spectrophotometric: 4.42 ± 0.04; NMR: 4.28 ± 0.05). Therefore,

Table 2. For compound **1** the Stern–Volmer constants K_{SV} are calculated with different anions, by the fitting of the I_0/I versus [anion] data with the Stern–Volmer Equation (2).

Anion	**1**/logK_{SV}	**2**/logK_{SV}[a]	**2**/logK_{ass}[a]	**2**/logK_{SV}[b]	**2**/logK_{ass}[b]	ρ
Cl^-	2.99 ± 0.03			3.16 ± 0.02	4.60 ± 0.04	0.71 ± 0.01
NO_3^-	2.86 ± 0.02			2.26 ± 0.06	3.87 ± 0.01	0.31 ± 0.01
HSO_4^-	1.27 ± 0.02			2.83 ± 0.06	3.78 ± 0.06[c]	0.98 ± 0.04
Br^-	3.04 ± 0.04	–	4.55 ± 0.05			
I^-	3.16 ± 0.04	4.09 ± 0.03	3.48 ± 0.01[c]			
NCS^-	3.16 ± 0.03	3.91 ± 0.05	3.40 ± 0.02[c]			

[a] Equation (3) was applied. [b] Equation (4) was applied; Equation (4) also contains the parameter ρ, whose refined values are obtained from the fitting. [c] In some cases, the spectrophotometrically determined K_{ass} values were employed in the fitting as fixed parameters.

we are not able to determine the K_{SV} value for the Br^-/**2** interaction.

The second case we consider is that the 1:1 adduct itself is fluorescent (i.e., the emission of the receptor–fluorophore has not been completely quenched by the included anion). If we define ρ as the residual fluorescence of the 1:1 adduct, we can write Equation (4) (see Appendix for its derivation):

$$I_0/I = (1 + K_{ass}[Q])(1 + K_{SV}[Q])/(1 + \rho K_{ass}[Q]) \quad (4)$$

This situation is observed in the case of Cl^-.

Figure 7 displays the I_0/I versus [Cl^-] data, which fit Equation (4) very satisfactorily. Corresponding values of K_{SV} and K_{ass} are reported in Table 2. The K_{ass} values are in good

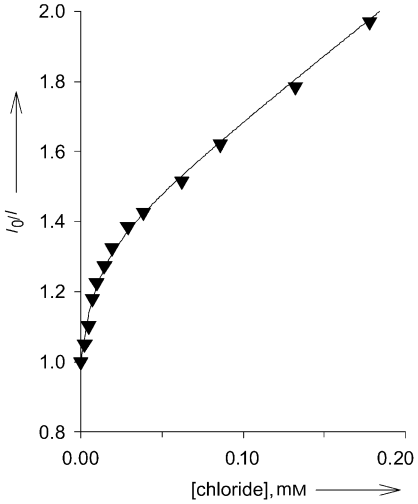

Figure 7. I_0/I versus [Cl^-] profile for the spectrofluorimetric titration of **2** with chloride. The curve was fitted by Equation (4) and the pertinent parameters are reported in Table 2.

agreement with those reported in Table 1. Notice that the calculated residual fluorescence ρ is 0.7. This means that the Cl^- ion included in the cavity is able to quench only 30% of the overall fluorescence of **2**.

A similar behaviour is displayed by NO_3^- and HSO_4^-; for both the anions, the formation of the adduct with **2** causes just partial quenching of the emission intensity. The fitting of the titration data by Equation (4) leads to the calculation of the residual fluorescence intensity ρ and both K_{SV} and K_{ass}. The calculated results are reported in Table 2.

The general behaviour is summarised in Figure 8, where I_0/I values versus [anion] are reported for both **1** and **2** and for all the investigated anions. The following features have to be remarked: 1) compound **2** is much more anion sensitive than **1**; this is a result of the combination of K_{SV}, generally higher for **2** than for **1**, and of K_{ass}, which allows a permanent contact between fluorophore and quencher; 2) compound **2** displays the highest response to Br^-, as a consequence of the especially high value of K_{ass}. The Cl^- ion shows an even higher association constant, but inside the inclusion complex it quenches only 30% of the fluorescence of **2**. Besides, chloride presents a relatively low value of K_{SV}, not far from the one observed for **1**.

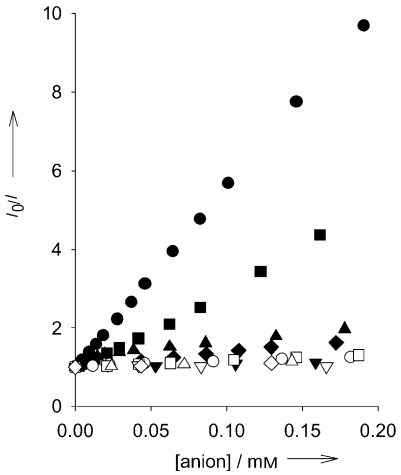

Figure 8. Profiles of I_0/I versus [anion] for both **1** (open symbols) and **2** (filled symbols) are reported. The same symbol shape is used to indicate the titration profile of **1** and **2** with the same anion (circles: Br^-; squares: I^-; triangles up: Cl^-; triangles down: HSO_4^-; diamonds: NO_3^-).

Conclusion

Quenching of simple fluorophores can be used for the determination of a variety of analytes, in particular anions, by benefitting from the Stern–Volmer equation, which correlates the fluorescence intensity to the concentration of the quenching analyte. We have demonstrated that organisation of the fluorogenic fragments in an appropriate geometrical array may generate a receptor capable of firmly interacting with the anionic subtrate, giving rise to an inclusion complex. This new situation astonishingly enhances the fluorimetric response, increasing the sensitivity by several orders of magnitude. Hence, in principle, selective or specific fluorophores can be designed for any desired anionic guest by choosing appropriate combinations of K_{ass} and K_{SV}. High values of K_{ass} can be obtained by synthesising receptors that display selective interaction with the envisaged anion, possibly introducing some rigidity in the molecular framework and modulating shape and size of the cavity. On the other hand, suitable values of K_{SV} can derive from the choice of fluorogenic fragments to be incorporated in the receptor. In this context, tens of fluorophores are waiting on the shelf (or in the chemical catalogues) to be chosen. In the very end, the design of a fluorescent receptor, characterised by convenient values of K_{ass} and K_{SV}, will lead to the achievement of analytically useful and especially sensitive I_0/I versus [anion] plots of the type illustrated in this work.

Experimental Section

General procedures and materials: All reagents were purchased from Aldrich/Fluka and used without further purification. Spectrophotometric and spetrofluorimetric grade solvents were used for spectroscopic measurements.

UV/Vis spectra were recorded on a Varian CARY 100 spectrophotometer, with a quartz cuvette (path length: 0.1 cm); spectrofluorimetric measurements were carried out on a Perkin–Elmer LS-50 luminescence spec-

trometer, using quartz sample tubes (path length: 1 cm). NMR spectra were recorded on a Bruker Avance 400 spectrometer, operating at 9.37 T.

Spectrophotometric titrations were performed at 25 °C on 5×10^{-4} M solutions of the ligand (**1** or **2**) in MeCN. Aliquotes of a fresh R_4NX (R = alkyl) standard solution were added and the UV/Vis spectra of the sample were recorded. All spectrophotometric titration curves were fitted with the HYPERQUAD program.[8] Spectrofluorimetric titrations were carried out by adding a standard solution of the anion to a 2×10^{-6} M solution of the ligand (the experiments were also repeated at higher concentration, 10^{-5} M). In each spectrofluorimetric titration, the excitation of the sample was performed at the wavelength value at which only negligible variations of absorbance occurred.

^{1}H NMR titrations were carried out as described before, but using CD_3CN as the solvent and working with high concentrations of the receptor ($>7\times10^{-4}$ M).

Synthesis of 1: MeI (0.12 mL, 1.9 mmol) was added to a solution of 6-methoxyquinoline (0.3 g, 1.88 mmol) in dry $CHCl_3$ (5 mL). The mixture was then heated at reflux for 1 h, under a dinitrogen atmosphere. A yellow solid (**1**·I^-) was collected by filtration and washed with several portions of Et_2O. The crude product was dissolved in hot water and treated with an aqueous saturated solution of NH_4PF_6. **1**·PF_6^- precipitated as a white solid (0.41 g, 77 %). ^{1}H NMR (400 MHz, CD_3OD, TMS): $\delta = 9.15$ (d, 1H, arom.), 9.08 (d, 1H, arom.), 8.42 (d, 1H, arom.), 8.01 (dd, 1H, arom.), 7.90 (dd, 1H, arom.), 7.80 (d, 1H, arom.), 4.68 (s, 3H, N^+–CH_3), 4.10 ppm (s, 3H, O–CH_3); elemental analysis calcd (%) for $C_{11}H_{12}NOPF_6$ (319.1): C 41.40, H 3.79, N 4.38; found: C 41.05, H 3.90, N 4.23.

Synthesis of 2: A solution of 6-methoxyquinoline (0.3 g, 1.9 mmol) in acetonitrile (20 mL) was added dropwise to a refluxing solution of 2,4,6-tris-(bromomethyl)mesitylene (0.2 g, 0.5 mmol) in acetonitrile (40 mL). The reaction was followed by TLC (silica gel, CH_2Cl_2/MeOH 8:0.5; $R_f = 0.1$). After 24 hrs at reflux, the solvent was removed by rotary evaporation and the crude product was washed with CH_3CN, then with Et_2O and purified by recrystallisation. Anion exchange yielded 0.35 g (65 %) **2**·$3PF_6^-$. ^{1}H NMR (400 MHz, CD_3OD, TMS): $\delta = 9.11$ (d, 1H, arom.), 8.77 (d, 1H, arom.), 8.75 (d, 1H, arom.), 8.08 (dd, 1H, arom.), 8.01 (dd, 1H, arom.), 7.88 (d, 1H, arom.), 6.40 (s, 2H, N^+–CH_2), 4.10 (s, 3H, O–CH_3), 2.28 ppm (s, 3H, Ar–CH_3); elemental analysis calcd (%) for $C_{42}H_{42}N_3O_3P_3F_{18}$ (1071.4): C 47.08, H 3.95, N 3.92; found: C 46.80, H 4.15, N 3.73.

Appendix

Derivation of the equations for the fluorescence intensity in the presence of dynamic quenching and partial static quenching: The here reported approach considers the possibility for the molecule M to form, at the ground state, a 1:1 complex (MQ) with the non-fluorescent species Q. Both M and MQ are fluorescent and both excited states (M* and MQ*) undergo dynamic quenching by species Q, according to Scheme 1, in which (M*···Q) and (MQ*····Q) are the pair between Q and M* and MQ* responsible for the dynamic quenching.

The decay of species M* and MQ* are described by the Equations (1a) and (2a):

$$\frac{d[M^*]}{dt} = -\left(\frac{1}{\tau_0} + k_Q[Q]\right)[M^*] = -\frac{1 + k_Q\tau_0[Q]}{\tau_0}[M^*] = -\frac{1 + K_{SV}[Q]}{\tau_0}[M^*] \quad (1a)$$

$$\frac{d[MQ^*]}{dt} = -\left(\frac{1}{\tau_0'} + k_Q'[Q]\right)[MQ^*] = -\frac{1 + k_Q'\tau_0'[Q]}{\tau_0'}[MQ^*] = -\frac{1 + K_{SV}'[Q]}{\tau_0'}[MQ^*] \quad (2a)$$

in which τ_0 and τ_0', k_Q and k_Q', K_{SV} ($=k_Q\times\tau_0$) and K_{SV}' ($=k_Q'\times\tau_0'$) are the excited state lifetimes, the dynamic quenching rate constants and the Stern–Volmer constants for the species M and MQ, respectively. Both equations were formulated by applying the Stern–Volmer approach[1] and considering the quenching rate constants as time-independent. The steady-state fluorescence intensity of species M ($I_{f(M)}$) and MQ ($I_{f(MQ)}$) are directly proportional to their concentration and inversely proportional to their observed lifetime in the presence of quencher [Eqs. (3a) and (4a)]:

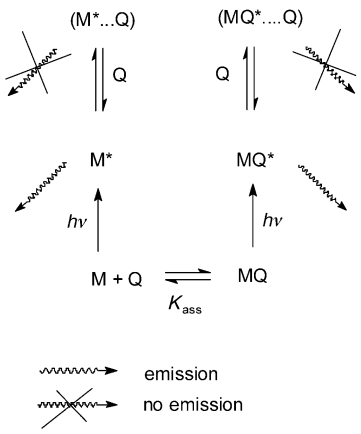

Scheme 1.

$$I_{f(M)} \propto \frac{\tau_0}{1 + K_{SV}[Q]}[M] \quad (3a)$$

$$I_{f(MQ)} \propto \frac{\tau_0'}{1 + K_{SV}'[Q]}[MQ] \quad (4a)$$

$[M_T]$ is the total concentration of the fluorescent receptor **2** (i.e., $[M_T] = [M] + [MQ]$). From this, I_0, the steady-state fluorescence in the absence of Q, can be obtained from Equation (3a) considering that $[M] = [M_T]$ [Eq. (5a)]:

$$I_{f(M)} \propto \tau_0[M_T] \quad (5a)$$

In the presence of Q the global fluorescence intensity (I_f) is the sum of that of species M and MQ; thus, from Equations (3a)–(5a), Equation (6a) can be obtained:

$$\frac{I_f}{I_0} = \frac{I_{f(M)} + I_{f(MQ)}}{I_0} = \frac{1}{1 + K_{SV}[Q]}\frac{[M]}{[M_T]} + \frac{\tau_0'/\tau_0}{1 + K_{SV}'[Q]}\frac{[MQ]}{[M_T]} \quad (6a)$$

The ratio τ_0'/τ_0 can be indicated as the *relative fluorescence intensity* of species MQ and M, namely ρ. If M and MQ are at equilibrium, their concentration is ruled by the equilibrium constant (K_{ass}), [Q] and $[M_T]$. The total Q concentration ($[Q_T]$) is: $[Q_T] = [Q] + [MQ]$. Treating the fraction of Q bound to M as negligible with respect to free Q ($[MQ] \ll [Q]$), that is, considering a low affinity equilibrium, the mass balance gives rise to Equations (6b) and (6c):

$$\frac{[M]}{[M_T]} = \frac{1}{1 + K_{ass}[Q]} \quad (6b)$$

$$\frac{[MQ]}{[M_T]} = \frac{K_{ass}[Q]}{1 + K_{ass}[Q]} \quad (6c)$$

These can be substituted into Equation (6a) to give Equation (7a):

$$\frac{I_f}{I_0} = \frac{1}{1 + K_{ass}[Q]}\left(\frac{1}{1 + K_{SV}[Q]} + \frac{\rho K_{ass}[Q]}{1 + K_{SV}'[Q]}\right) \quad (7a)$$

Taking the I_0/I_f ratio, as in the Stern–Volmer relation, and assuming that the Stern–Volmer constants for M and for MQ do not differ significantly ($K_{SV} \approx K_{SV}'$) Equation (7a) can be reduced to Equation (8a):

$$\frac{I_0}{I_f} = \frac{(1 + K_{ass}[Q])(1 + K_{SV}[Q])}{1 + \rho K_{ass}[Q]} \quad (8a)$$

Within the approximation indicated (i.e., $[MQ] \ll [Q]$), Equation (8a) reproduces the fluorescence pattern reported in Scheme 1. It must be noted that when species MQ is not fluorescent ($\rho = 0$), Equation (8a) re-

duces to the simpler equation valid for the coupled static and dynamic quenching.[1]

This approach can be extended to the case in which the equilibrium constant (K_{ass}) is so high (high affinity limit) that the fraction of Q bound to M cannot be neglected in the mass balance. In this situation the relation $[Q]=[Q_T]-[MQ]$ must be explicitly considered in both dynamic quenching and ground state equilibrium. Applying the mass balance to M and on Q and considering the equilibrium constant K_{ass}, the concentrations at equilibrium are given by the Equations (9a)–(12a):

$$[MQ] = \frac{K_{ass}([M_T]+[Q_T])+1-R}{2K_{ass}} \quad (9\,a)$$

$$[M] = \frac{K_{ass}([M_T]-[Q_T])-1+R}{2K_{ass}} \quad (10\,a)$$

$$[Q] = [Q_T]-\frac{K_{ass}([M_T]+[Q_T])+1-R}{2K_{ass}} \quad (11\,a)$$

$$R = \sqrt{K_{ass}^2([M_T]-[Q_T])^2+2K_{ass}([M_T]+[Q_T])+1} \quad (12\,a)$$

The ratio I_0/I_f can be obtained upon substitution of Equations (9a)–(11a) into Equation (6a) and assuming again that $K_{SV}\approx K'_{SV}$ [Eq. (13a)]:

$$\frac{I_0}{I_f} = [M_T]\frac{2K_{ass}+K_{SV}[K_{ass}([Q_T]-[M_T])-1+R]}{2K_{ass}[M_T]+(\rho-1)[K_{ass}([Q_T]+[M_T])+1-R]} \quad (13a)$$

Equation (13a) differs from Equation (8a), because the shape of the I_0/I_f versus $[Q_T]$ curve depends on the initial M concentration. However, it should be noted that for $K_{ass}\rightarrow 0$ or $[M_T]\rightarrow 0$ Equation (13a) can be reduced to Equation (8a). Equation (13a) can also be applied when MQ is not fluorescent, by simply using $\rho=0$.

Acknowledgement

The financial support of the European Union (RTN Contract HPRN-CT-2000-00029) and the Italian Ministry of University and Research (PRIN - Dispositivi Supramolecolari) is gratefully acknowledged.

[1] B. Valeur, *Molecular Fluorescence, Principles and Applications*, Wiley-VCH, Weinheim, **2002**.
[2] S. Jayaraman, A. S. Verkman, *Biophys. Chem.* **2000**, *85*, 49.
[3] C. D. Geddes, K. Apperson, J. Karolin, D. S. Birch, *Anal. Biochem.* **2001**, *293*, 60.
[4] F. P. Schmidtchen, M. Berger, *Chem. Rev.* **1997**, *97*, 1609.
[5] A. Bianchi, K. Bowman-James, E. García-España, *Supramolecular Chemistry of Anions*, Wiley-VCH, New-York, **1997**.
[6] S. L. Wiskur, H. Ait-Haddou, J. J. Lavigne, E. V. Anslyn, *Acc. Chem. Res.* **2001**, *34*, 963.
[7] L. O. Abouderbala, W. J. Belcher, M. G. Boutelle, P. J. Cragg, J. Dhaliwal, M. Fabre, J. W. Steed, D. R. Turner, K. J. Wallace, *Chem. Commun.* **2002**, 358.
[8] P. Gans, A. Sabatini, A. Vacca, *Talanta* **1996**, *43*, 1739.
[9] Hyperchem 6.0. Molecular Modeling System. Hypercube Inc.
[10] K. J. Wallace, W. J. Becher, D. R. Turner, K. F. Syed, J. W. Steed, *J. Am. Chem. Soc.* **2003**, *125*, 9699.
[11] B. Valeur, *Molecular Fluorescence, Principles and Applications*, Wiley-VCH, Weinheim **2002**, p. 73.
[12] H. Shizuka, M. Nakamura, and T. Morita, *J. Phys. Chem.* **1980**, *84*, 989.
[13] B. Valeur, *Molecular Fluorescence, Principles and Applications*, Wiley-VCH, Weinheim, **2002**, p. 86.

Received: July 15, 2003 [F5338]